the plant journal

SEB SOCIETY FOR EXPERIMENTAL BIOLOGY

The Plant Journal (2024) doi: 10.1111/tpj.16945

MatK impacts differential chloroplast translation by limiting spliced tRNA-K(UUU) abundance

Jose M. Muino[1,2], Hannes Ruwe[3,†], Yujiao Qu[3,†], Sascha Maschmann[3], Wei Chen[4,5], Reimo Zoschke[6], Uwe Ohler[2,*,§], Kerstin Kaufmann[1,*,§] and Christian Schmitz-Linneweber[3,*,§]

[1]*Plant Cell Development, Humboldt Universität zu Berlin, Philippstr.13, 10115 Berlin, Germany,*

[2]*Computational Regulatory Genomics, Humboldt-University Berlin/Max Delbrück Centre for Molecular Medicine, 10115 Berlin, Germany,*

[3]*Molecular Genetics, Humboldt Universität zu Berlin, Philippstr.13, 10115 Berlin, Germany,*

[4]*Department of Biology, Southern University of Science and Technology, Shenzhen, Guangdong, China,*

[5]*Medi-X Institute, SUSTech Academy for Advanced Interdisciplinary Studies, Southern University of Science and Technology, Shenzhen, Guangdong, China, and*

[6]*Max Planck Institute of Molecular Plant Physiology, Am Mühlenberg 1, 14476 Potsdam-Golm, Germany*

Received 26 February 2024; revised 10 July 2024; accepted 13 July 2024.

*For correspondence (e-mail uwe.ohler@mdc-berlin.de; kerstin.kaufmann@hu-berlin.de; christian.schmitz-linneweber@hu-berlin.de).

†These authors contributed equally to this work, respectively.

§These corresponding authors, have equally contributed as well among each other.

SUMMARY

The protein levels of chloroplast photosynthetic genes and genes related to the chloroplast genetic apparatus vary to adapt to different conditions. However, the underlying mechanisms governing these variations remain unclear. The chloroplast intron Maturase K is encoded within the *trnK* intron and has been suggested to be required for splicing several group IIA introns, including the *trnK* intron. In this study, we used RNA immunoprecipitation followed by high-throughput sequencing (RIP-Seq) to identify MatK's preference for binding to group IIA intron domains I and VI within target transcripts. Importantly, these domains are crucial for splice site selection, and we discovered alternative 5′-splice sites in three MatK target introns. The resulting alternative *trnK* lariat structure showed increased accumulation during heat acclimation. The cognate codon of tRNA-K(UUU) is highly enriched in mRNAs encoding ribosomal proteins and a *trnK-matK* over-expressor exhibited elevated levels of the spliced tRNA-K(UUU). Ribosome profiling analysis of the overexpressor revealed a significant up-shift in the translation of ribosomal proteins compared to photosynthetic genes. Our findings suggest the existence of a novel regulatory mechanism linked to the abundance of tRNA-K(UUU), enabling the differential expression of functional chloroplast gene groups.

Keywords: chloroplast, tRNA, translation regulation, splicing, intron maturase, IEP.

INTRODUCTION

Chloroplast genomes in land plants contain two main functional categories of genes: those that directly encode components of the photosynthetic apparatus (referred to as PS genes) and those that encode components of the genetic apparatus (referred to as GA genes). These two sets of genes have been shown to exhibit differential gene expression during leaf development. In maize, for example, the genes responsible for the ribosome and the RNA polymerase exhibit strong translation in the leaf base where proplastids are located and chloroplast biogenesis begins. Conversely, the translation of photosynthetic genes occurs at a later stage (Chotewutmontri & Barkan, 2016). Similar observations have been made in barley and Arabidopsis (Baumgartner et al., 1993; Emanuel et al., 2004; Zoschke et al., 2007). This expression pattern potentially aids in priming the gene expression apparatus in proplastids for the subsequent massive production of photosynthetic proteins.

The mechanistic basis of this differential translation remains unclear, but both transcriptional and post-transcriptional processes are known to play a role (Chotewutmontri & Barkan, 2016). It can be expected that the differential expression of these two gene groups is driven, at least in part, by differential transcription. Most GA genes possess promoters for a nuclear-encoded RNA

polymerase (NEP), whereas PS genes are predominantly transcribed by the plastid-encoded RNA polymerase (PEP). Although both RNA polymerases are active in various tissues, NEP-dependent activity is typically strong in young leaf tissue, whereas PEP is active throughout the leaf (Liebers et al., 2017). In addition to transcription, post-transcriptional processes, particularly translation, are believed to contribute significantly to the regulation of chloroplast genes (Zoschke & Bock, 2018).

Chloroplast RNA metabolism is characterized by various RNA processing events, including RNA cleavage, RNA editing, and RNA splicing (Small et al., 2023). This complexity is paralleled by the large number of RNA processing factors that have been identified to date. Several families of nuclear-encoded RNA binding proteins have evolved to specifically regulate plant organellar RNA metabolism (Small et al., 2023). More than 150 factors have been described as necessary for chloroplast RNA metabolism alone (Small et al., 2023). Apart from these nuclear-encoded factors, only one chloroplast-encoded putative RNA processing factor, named Maturase K (MatK), has been identified. MatK is related to bacterial intron maturases and is found in all chloroplast genomes of autotrophically growing land plants, as well as in charophycean green algae (Turmel et al., 2006). It is located within the *trnK* intron and is believed to be involved in splicing its own intron, similar to bacterial maturases. However, in certain species where the *trnK* gene is absent, such as streptophyte algae *Zygnema*, the fern *Adiantum capillus-veneris*, and parasitic land plants (*Epifagus virginiana*, several *Cuscuta* species), *matK* exists as an independent reading frame (Braukmann et al., 2013; Funk et al., 2007; McNeal et al., 2007; Turmel et al., 2005; Wolfe et al., 1992). The fact that the loss of *trnK* does not correspond to the loss of *matK* suggests that *matK* serves other functions and potentially targets different introns. Only *Rhizanthella gardneri*, a mycoheterotrophic orchid, and certain members of the *Cuscuta* subgenus of parasitic angiosperms have been observed to lack *matK*. These species have also lost several group IIA introns that may require the activity of MatK (Braukmann et al., 2013; Delannoy et al., 2011; McNeal et al., 2007). The available evidence supports the hypothesis that MatK is involved in splicing other introns, not just its own intron. This is further supported by studies on chloroplasts devoid of a translational apparatus, where the *trnK* precursor RNA is not spliced (Vogel et al., 1997) and in addition, an entire subgroup of chloroplast introns, termed group IIA introns, fails to splice as well (Hess et al., 1994; Vogel et al., 1999). The only plausible factor that would require functional chloroplast translation for splicing is MatK, leading to the proposition that MatK is responsible for splicing all group IIA introns. Indeed, MatK has been shown to interact with intron RNA both *in vitro* (Liere & Link, 1995) and *in vivo* (Zoschke et al., 2010), and recombinant MatK supports splicing in an *in vitro* splicing assay (Barthet et al., 2020).

Group II introns are characterized by six secondary structure elements, named domain DI–DVI, which fold into a globular tertiary structure (Michel & Ferat, 1995; Zhao & Pyle, 2017). Bacterial maturase reading frames, including *matK*, are always encoded within DIV. Bacterial maturases establish direct contacts with selected intron sequence elements, and these contacts are essential for the splicing reaction. For example, the bacterial Maturase LtrA interacts with sequence stretches within DI, DII, and DIV. These contacts contribute to the attainment of a splicing-competent intron conformation (Matsuura et al., 2001; Rambo & Doudna, 2004). However, little is known about the preferences of MatK for specific intron domains or how MatK supports intron splicing in living cells.

Functional genetic studies of MatK have been hindered so far by the inability to disrupt the chloroplast *matK* reading frame through various mutagenesis approaches. This suggests that *matK* may be an essential gene (Drescher, 2003; Zoschke et al., 2010). A natural mutation in MatK of *Cryptomeria japonica* remains heteroplastomic and leads to infrequent segregation of chlorophyll-deficient sectors, further supporting the notion that MatK is essential for chloroplast development and the survival of whole plant cells (Hirao et al., 2009). Similarly, ectopic expression of MatK from the tobacco chloroplast genome resulted in variegated plants with white sectors and impaired chloroplast development (Qu et al., 2018).

In this study, we identify the specific interaction sites of MatK with chloroplast introns and demonstrate that MatK is required for the correct branch-point selection of the *trnK* intron. Furthermore, we show that *trnK* production correlates with the translation of GA genes, which are rich in lysine codons. Overexpression of MatK induces increased GA translation, likely mediated by increased tRNA-K accumulation, a mechanism that appears to be relevant during heat acclimation.

RESULTS

Comprehensive analysis of binding sites within group IIA introns identifies a preference of MatK for domains I and VI

The resolution of prior RIP-Chip analyses investigating the RNA targets of the MatK protein was limited by probe size (Zoschke et al., 2010). To gain more precise insights into MatK binding sites within its target introns, we used RNA Immunoprecipitation Sequencing (RIP-Seq). To precipitate MatK, we utilized transplastomic *Nicotiana tabacum* plants expressing MatK with a C-terminal Hemagglutinin (HA) epitope tag (+HA), alongside a non-tagged control line (−HA) as previously described (Zoschke et al., 2010). The RNA co-precipitated with MatK was examined via RNA-seq, with

the objective to determine the MatK binding sites more precisely. In the chloroplast stroma, nucleolytic activity can fragment unprotected RNAs, leaving the RBP-bound RNA segments recovered in the pellet of the immunoprecipitation (Schmitz-Linneweber et al., 2005). These preserved fragments indicate the specific sites of association of the RBPs. The immediate treatment of the precipitated RNA-protein complexes with phenol-chloroform, used for RNA extraction, ensures that RNA degradation post-precipitation is minimized, further enhancing the accuracy of binding site identification. This process, therefore, provides a clear snapshot of the RNA sequences directly interacting with the protein, pinpointing the specific sites of RNA association.

In light of the fact that MatK protein expression peaks in 7-day-old tobacco plants (Zoschke et al., 2010), we isolated chloroplasts from seedlings of this exact age for our analysis. Moreover, given that MatK is a soluble protein located in the chloroplast stroma (Zoschke et al., 2010), we separated the stroma fraction from the membrane fraction to increase the concentration of MatK protein. Consequently, immunoprecipitation (IP) was carried out using the stroma fraction, with the effectiveness of this approach confirmed through immunoblot analysis (Figure 1a). We then extracted and sequenced the RNA co-precipitated with MatK from three independent biological replicates, and determined the relative enrichment compared to IPs from −HA plants. As anticipated, the most pronounced relative enrichment was observed for the already known intron targets of MatK (Figure 1b; Table S1; Zoschke et al., 2010; the intron in *trnV(UAC)* is an exception as it does not appear to be enriched here). There were no peaks for RNAs containing other intron types or for RNAs containing no intron at all (Figure 1b), confirming the known specificity of MatK (Zoschke et al., 2010).

The different intron domains fulfill different functions in the splicing process and it is therefore informative to assign binding of MatK to individual domains. Thus, we centered our analysis on the enrichment of RNA across the different intron domains (Figure 1c). Visual inspection of enrichment pointed to domain I and the 3′-terminal domain VI as frequent targets of MatK in almost all introns. For domain I, in most cases peak enrichment is near the immediate 5′-end of the domain as well as in the center of the domain. Additional target sites are found in the other domains (e.g. domain II for *atpF*), but these are not showing higher enrichment compared to binding sites within domains I and VI. Finally, there are binding sites in the second exon of most targets. Since the exons are very short for the four tRNA targets, it is possible that there is simply co-enrichment with domain VI, since the longer second exons of *atpF* and *rpl2* do only show enrichment right adjacent to domain VI within the intron and at much lower enrichment value (Figure 1c).

We next quantified the peak enrichment within each domain—we calculated the mean of the forty bases with the highest enrichment value for each domain and translated this into a heat map (Figure 1d). This focus on top peak height in each domain also avoids the introduction of a length bias, which otherwise leads to an artificial overrepresentation of domain I. We clustered the domains and found that domains I and VI are most similar in their enrichment across all introns and show highest enrichment for most introns. Although there appears to be flexibility in target site preferences between introns, our findings indicate a predilection of MatK toward domains I and VI.

Identification of alternative lariat formation in chloroplast introns

Domain VI, a primary target of MatK, plays a crucial role in splicing chemistry. It houses the looped-out adenosine that serves as the branch point during the first splicing phase (Pyle, 2016; Vogel & Börner, 2002). The selection of the branch point is governed by the structural positioning of Domain VI (DVI) within the group II intron holostructure. This positioning depends on the interactions of exon binding sites in Domain I (DI) that base-pair with exon sequences, thereby aligning the 5′-splice site with the branch point (Zhao & Pyle, 2017). In spliceosomal introns, which have evolved from group II introns, branch point selection relies on the recognition of sequence context by RNA binding proteins and small nuclear ribonucleoproteins (snRNPs). This process can vary, leading to alternative branch points.

We screened published standard total RNA-seq datasets from tobacco (Grimes et al., 2014) and Arabidopsis (Zhang et al., 2019) for reads that could help to identify the exact branch point position, thereby determining the possibility of alternative branch points. Such reads would originate immediately downstream of the 5′-splice site and continue across the 2′- to 5′-phosphodiester linkage at the branch point into the 3′-sequence of the intron (Figure 2a). Our analysis of RNA-seq data from tobacco, Arabidopsis identified such reads, representing the expected 5′-splice site to known branch point connections for introns in *trnG-UCC*, *petD*, and the two introns in *ycf3* (Figure 2b). Unexpectedly, we also discovered alternative lariats for the introns *trnK*, *trnA*, and *atpF*, all of which are MatK targets (Figure 2c).

For *trnK* and *trnA*, these alternative lariats utilize 5′ splice sites downstream of the canonical site, 374 nt inside the intron from the intron's canonical 5′-end. The branch point A, however, is preserved in the alternative lariats of *trnK* for both investigated plant species and for *trnA* in tobacco, with only the 5′-splice site changing. This contrasts with *trnA* in *Arabidopsis*, where we identified an alternative lariat formed through an alternative branch point within exon 2. In the *atpF* intron, the branch point

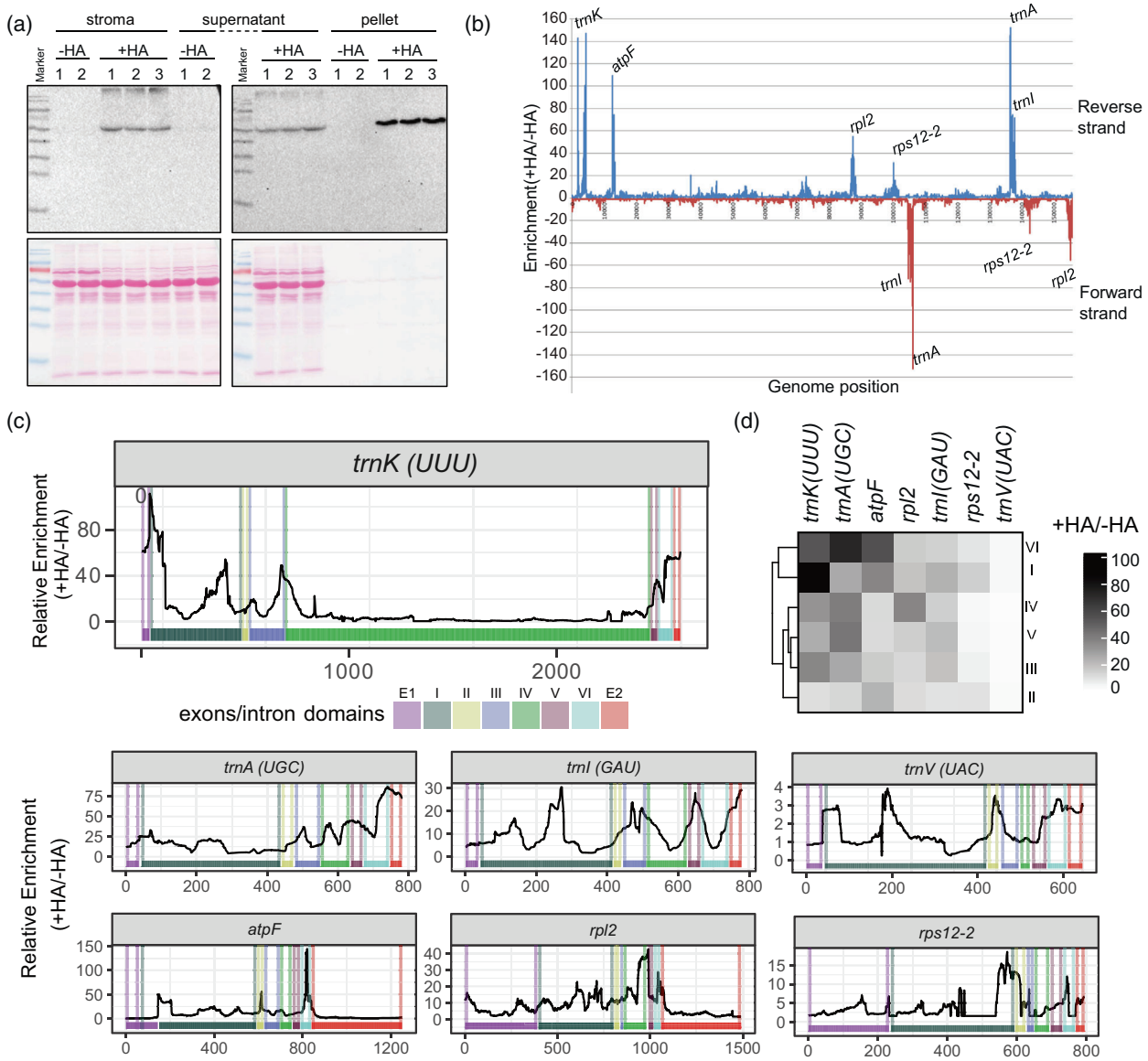

Figure 1. Immunoprecipitation of HA-tagged MatK from transplastomic tobacco lines.

(a) Chloroplasts were obtained from 7-day-old tobacco seedlings expressing either the HA-tagged MatK (+HA) or the non-tagged control (−HA). Immunoprecipitation of the chloroplast stroma was performed using an HA antibody (Sigma) and magnetic beads (Life Technologies). The protein samples, including the input, IP supernatant, and IP pellet, were separated using SDS-PAGE gel and transferred to a nitrocellulose membrane. HA-specific signals were detected using an HA antibody (upper panel). Ponceau staining was utilized as a loading control (lower panel). The band's position at about 55 kDa aligns with previous immunological studies on MatK (Barthet & Hilu, 2007; Liere & Link, 1995; Zoschke et al., 2010).

(b) Comprehensive mapping of MatK targets identified through RIP-seq. RNA samples from the IP pellets of three independent +HA IP experiments and two independent −HA experiments were used to generate libraries, which were subsequently sequenced. The resulting reads from each library, corresponding to the +HA and −HA tagged MatK-IP pellets, were normalized, averaged and mapped to the chloroplast genome (NC_001879). The ratio of mapped reads between the +HA and −HA samples was calculated and plotted onto the chloroplast genome. Peak enrichments are labeled with gene names.

(c) Close-up view of the MatK targets identified through RIP-seq. The reads from the +HA and −HA tagged MatK libraries were separately aligned to the chloroplast genome (NC_001879), and the ratio of mapped reads between the +HA and −HA samples was calculated and plotted along the chloroplast genome sequence of the genes shown. The *trnK* plot is enlarged relative to the other introns shown since the intron is far longer because of the *matK* reading frame being positioned within intron domain IV. The bar below the graph indicates the distribution of exons and domains of group II introns, as previously defined (Michel et al., 1989).

(d) Relative enrichment of each domain of MatK associated RNAs based on RIP-Seq analysis. For each MatK-associated intron, the twenty bases with the highest relative enrichment for each domain were selected and a mean enrichment value (+HA/−HA) was calculated and transformed into a heat map. Based on these peak enrichment values, the domains were clustered using Euclidean distance, complete linkage.

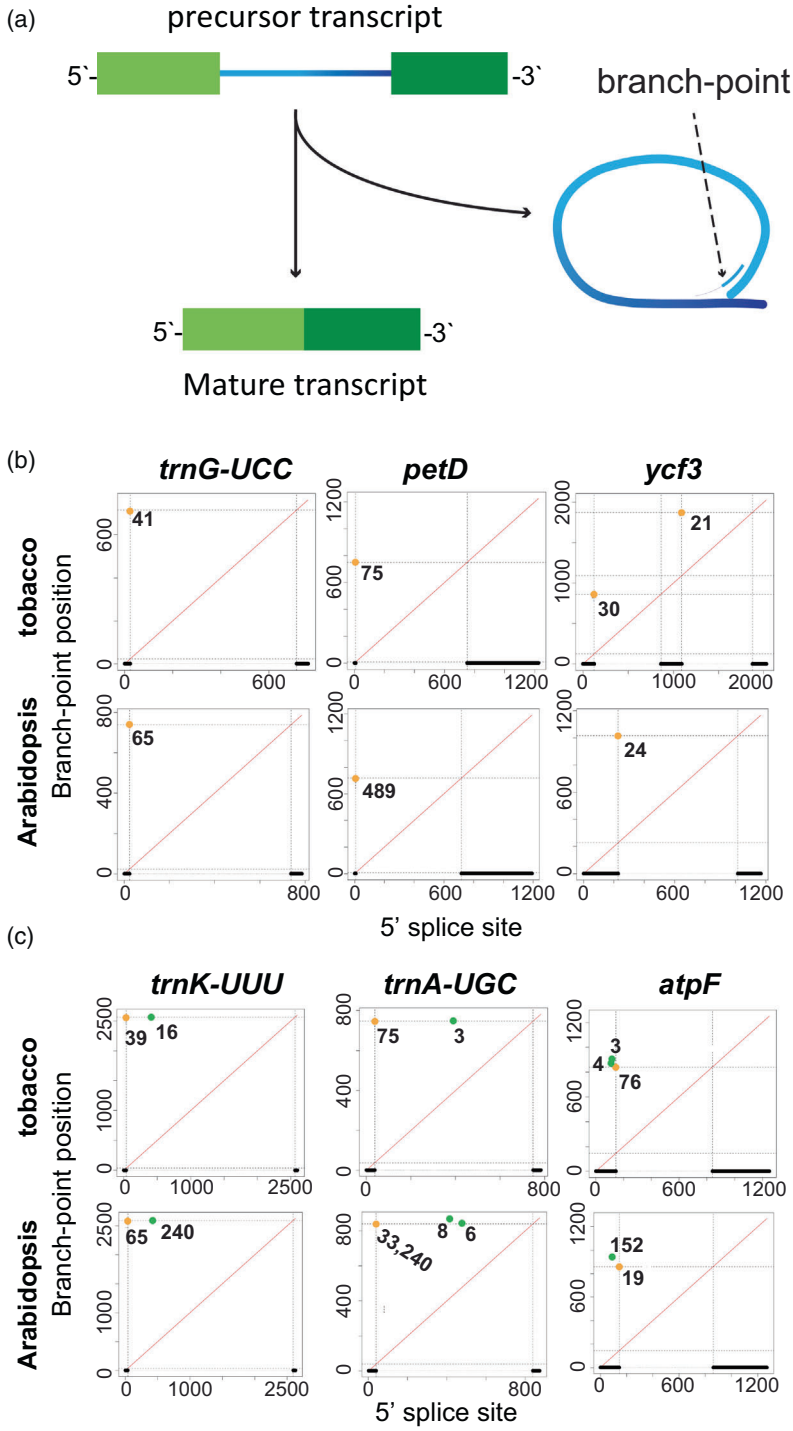

Figure 2. Lariat detection in chloroplast introns in RNA-seq data.
(a) Graphic representation of reads spanning the 2′-to-5′ bridge at branch-points within lariats. Light green: 5′-exon; dark green: 3′-exon. blue: intron (different hues of blue are used to allow easy differentiation between the 5′-end and 3′-end of the intron).
(b) RNA-seq data from tobacco or Arabidopsis were screened for informative reads spanning the 2′-to-5′ bridge at branch-points within lariats. Introns with canonical branch points only: Mapping of branch point reads relative to 5′ splice acceptor sites in tobacco and Arabidopsis. Thick lines at the bottom of the figure indicate exon positions with connecting thin dotted lines representing the borders of the intron. Numbers indicate branch point reads found in the combined RNA-seq datasets. Numbers at axis refer to position relative first base of exon 1. Canonical branch points are shown in orange.
(c) Introns with alternative branch points: as in (b), but with alternative branch points shown in green.

The Plant Journal published by Society for Experimental Biology and John Wiley & Sons Ltd.,
The Plant Journal, (2024), doi: 10.1111/tpj.16945

also shifted into exon 2 and the 5′-splice site moved into exon 1, resulting in a longer excised intron.

As an alternative method to verify the existence of alternative lariats and test for their abundance, we used an RNase R assay. RNase R, a 3′-to-5′ exonuclease, can degrade non-branched precursors but is incapable of degrading lariats across the branch point (Suzuki et al., 2006). We analyzed RNase R treated total RNA through RNA gel blot hybridization using a probe for the *trnK* intron. This intron has the highest number of reads representing alternative lariats compared to canonical ones (Figure 2b). We analyzed RNA from both wild-type (wt) tobacco plants and a line that exhibits increased *matK* expression. This line, named 5′+HA, possesses an *aadA* selection marker cassette upstream of the *trnK* gene, with a 5′-extension of the *matK* reading frame encoding a Hemagglutinin (HA)-tag (Zoschke et al., 2010). This cassette is powered by the robust 16S rRNA promoter, which leads to readthrough into the downstream *trnK* gene, as indicated by an additional band of about 5 kb absent in the wt (Figure 3). Additional evidence supporting overexpression will be presented subsequently.

Unspliced RNAs were detected using an exon 2 probe, revealing a major band of approximately 2.6 kb and a strong signal corresponding to the spliced, mature tRNA-K (Figure 3a). In contrast, we were unable to detect a signal for the alternatively spliced product, expected to be 446 nucleotides long. We speculate that either the alternative lariat does not successfully participate in a productive second splicing step, or the abnormally long product is quickly degraded. The 2.6 kb signal for the linear *trnK* precursor RNA is entirely removed by RNase R treatment. The mature tRNA is enriched, as tRNAs are not an ideal substrate for RNase R (Suzuki et al., 2006), whereas rRNAs are also degraded efficiently (see Methylene blue stain below autoradiograms in Figure 3a). Conversely, using an intron-specific probe, we identified two transcripts that resist RNase R treatment, matching in size to the canonical and alternative lariats. However, it should be noted that circular lariat RNAs will migrate differently through a gel, preventing precise size determination. Together, the RNA-seq and RNA gel blot experiments confirm the existence of two alternative lariats originating from the *trnK* precursor RNA.

Alternative splicing in the nucleus is a highly regulated process that responds to various external cues. To test whether alternative lariat formation is also reacting to environmental changes, we checked the accumulation of

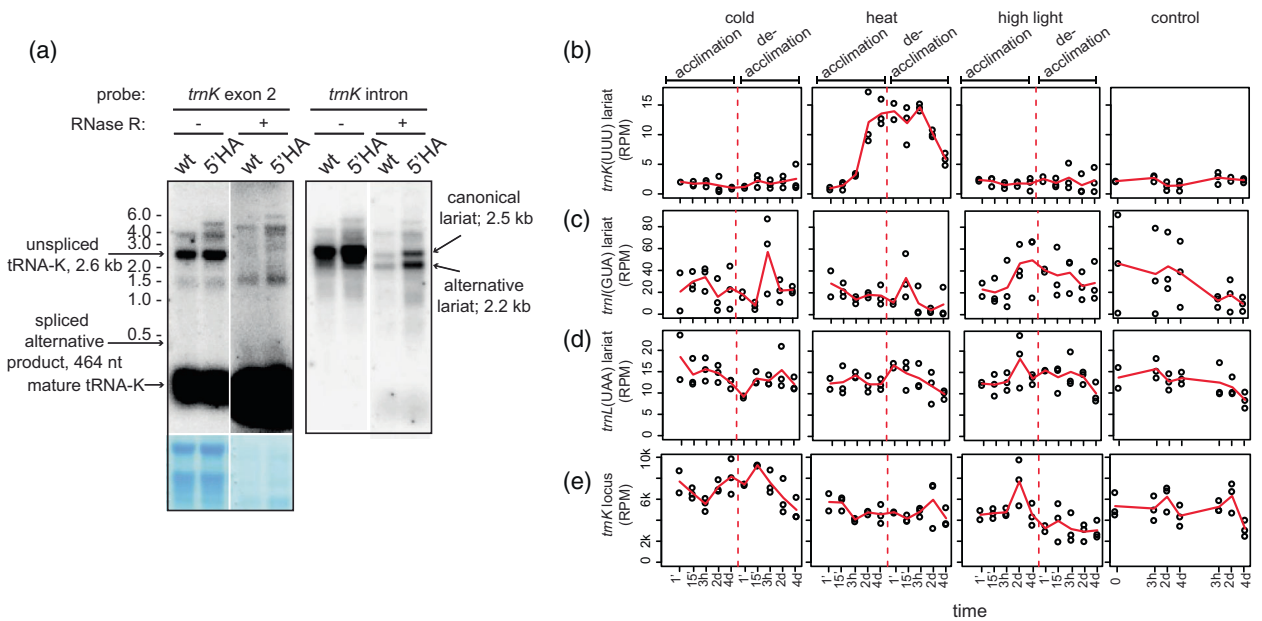

Figure 3. Accumulation of two *trnK* lariat isoforms.
(a) 5 μg of total plant RNA was either directly analyzed by RNA gel blot hybridization or after treatment with RNase R. Left: hybridization with a probe against exon 2 of *trnK;* methylene blue staining of the RNA gel blot to indicate equal loading. The white line indicates the removal of the marker lane and other lanes not relevant. Right: after stripping of the exon probe, a *trnK* intron probe was hybridized to the same membrane.
(b) Analysis of RNA-seq reads representing the alternative *trnK* lariat isoform and canonical lariats in a dataset for cold, heat and high light acclimation (Garcia-Molina et al., 2020). The dashed red line indicates the last sample taken in the initial acclimation phase before plants were put back to standard growth conditions for de-acclimation.
(c) Same as in (b), but for *trnI*(GUA).
(d) Same as in (b), but for *trnL*(UAA).
(e) Analysis of all RNA-Seq reads representing the *trnK* precursor RNA from the same dataset as used in (b) and (c). Note that the increase in lariat reads during heat acclimation (b) is not reflected in an increase of precursor RNA.

the lariat in recently published RNA-seq datasets for *Arabidopsis thaliana* (Garcia-Molina et al., 2020). We were using data from a study that exposed plants to mild changes in abiotic conditions requiring acclimation, but not yet exhibiting stress. The study used exposure to high light at 450 μmol photons m^{-2} sec^{-1}, cold exposure to 4°C, and heat exposure to 32°, all independently for 4 days, with subsequent de-acclimation for 5 days (Garcia-Molina et al., 2020). In these datasets, we counted branch point reads for the alternative *trnK* lariat (Figure 3b; reads for the canonical lariat are very rare) and also counted lariat reads for two further intron-containing tRNAs (Figure 3c,d). Neither in cold nor in high light did we find any pronounced changes in the accumulation of these lariats, with maybe a possible slight increase in alternative tRNA-I lariats during high light acclimation (Figure 3b–d). In heat acclimation however, a more than 7-fold increase in the alternative lariat was observed after 3 days of high temperature exposure that persisted for a few hours after return to regular growth temperature before it declined at the latest time points of de-acclimation (Figure 3b). The two other introns did not show such an increase in lariat reads. Also, the *matK* locus itself does not show increased expression during heat acclimation (Figure 3e). This indicates that heat is a specific modifier of *trnK* splicing that increases the formation and/or stability of the alternative lariat.

The lysine codon read by tRNA-K differentiates between ribosomal and photosynthetic genes

To discern whether there is a bias in the distribution of the AAA codon read by tRNA-K(UUU) in different chloroplast genes, we conducted a hierarchical cluster analysis of all chloroplast protein-coding genes from tobacco based on their codon usage (Figure 4a). Codon bias was calculated from the sequence of each protein coding plastid gene independently. The number of each codon was calculated for each gene and divided by the total number of codons of this particular gene. Two main clusters were found depending on their codon composition, which corresponded mainly to photosynthetic genes versus ribosomal genes. Figure 4a further indicates that the lysine codon, AAA, is the main driver of this clustering, as it showed a significant (P value $<1.7 \times 10^{-9}$, t-test) higher frequency in genes that code for ribosomal proteins, than encoding photosynthetic proteins. Furthermore, the codons for basic amino acids, specifically CGT, CGA, AGA (arginine) and AAG (lysine), are also overrepresented in genes encoding ribosomal proteins. The codon AAG for lysine is likely accommodated by tRNA-K(UUU) through wobble base pairing, given that this is the sole lysine tRNA in the chloroplast, and there is no evidence to suggest the import of tRNAs into chloroplasts thus far.

Building on this discovery, we directly compared the codon frequencies in ribosomal protein genes versus photosynthesis genes. The AAA codon emerged as the most biased codon, with a marked preference for ribosomal protein genes (Figure 4b). Given their function in binding rRNA, ribosomal proteins are known to be rich in positively charged amino acids, which generally necessitates a high presence of lysine codons. Although the same could be expected for arginine codons, we observed no such bias for arginine codons AGG, CGC and CGG, and only a mild overrepresentation of CGT, CGA, AAG and AGA codons in ribosomal protein genes. Considering the AT-rich nature of chloroplast genomes, a predilection for AAA codons could be partly explained by selection for AT-rich codons. However, the AAA codon certainly distinguishes between ribosomal and photosynthetic genes, leading us to hypothesize that this gene-group-specific bias might have regulatory implications. Intriguingly, the TTT codon, which codes for phenylalanine, displayed an opposite bias, being overrepresented in photosynthetic genes. Next, to investigate the potential importance of the AAA codon for the differential translation of gene groups, we sought methods to manipulate the levels of tRNA-K(UUU).

Enhanced levels of mature tRNA-K in 5′+HA transplastomic plants

Among the two alternative branch point pathways for *trnK* that we identified, only one results in the production of mature tRNA-K. The alternative lariat pathway would fuse a significantly longer first exon to a standard second exon, which would lead to a nonfunctional tRNA (Figure S1). However, we couldn't detect this elongated tRNA in our RNA gel blots (Figure 3, exon probe hybridization), suggesting that the second splicing step may either be unsuccessful or the product is quickly degraded.

We next asked whether there is a correlation between the expression levels of the *trnK* precursor/*matK* mRNA and the production of functional tRNA-K. We decided to explore this by using the previously generated transplastomic lines (Zoschke et al., 2010) that have *aadA* cassettes upstream or downstream of the *matK* reading frame, either with or without a triple HA-tag added to the coding sequence (Figure 5a). We used RNA gel blot hybridization to analyze the expression of *matK* in these lines. The 5′+HA line exhibits a significantly increased accumulation of the *trnK*-precursor relative to the wild-type (Figure 5b,c). Surprisingly, this is not observed for the 5′−HA transplastomic line, suggesting that the presence of the HA-tag sequence enhances *trnK* precursor stability—for unknown reasons. Relevant for the further analysis, the 5′+HA transplastomic line over-expresses the *trnK* precursor, essentially serving as an over-expressor of the *matK* mRNA. By contrast, both lines carrying the *aadA* cassette 3′ to the *trnK* gene do not show alterations in precursor RNA accumulation, which is expected given that the 3′-cassettes cannot contribute to transcription of the *trnK* locus.

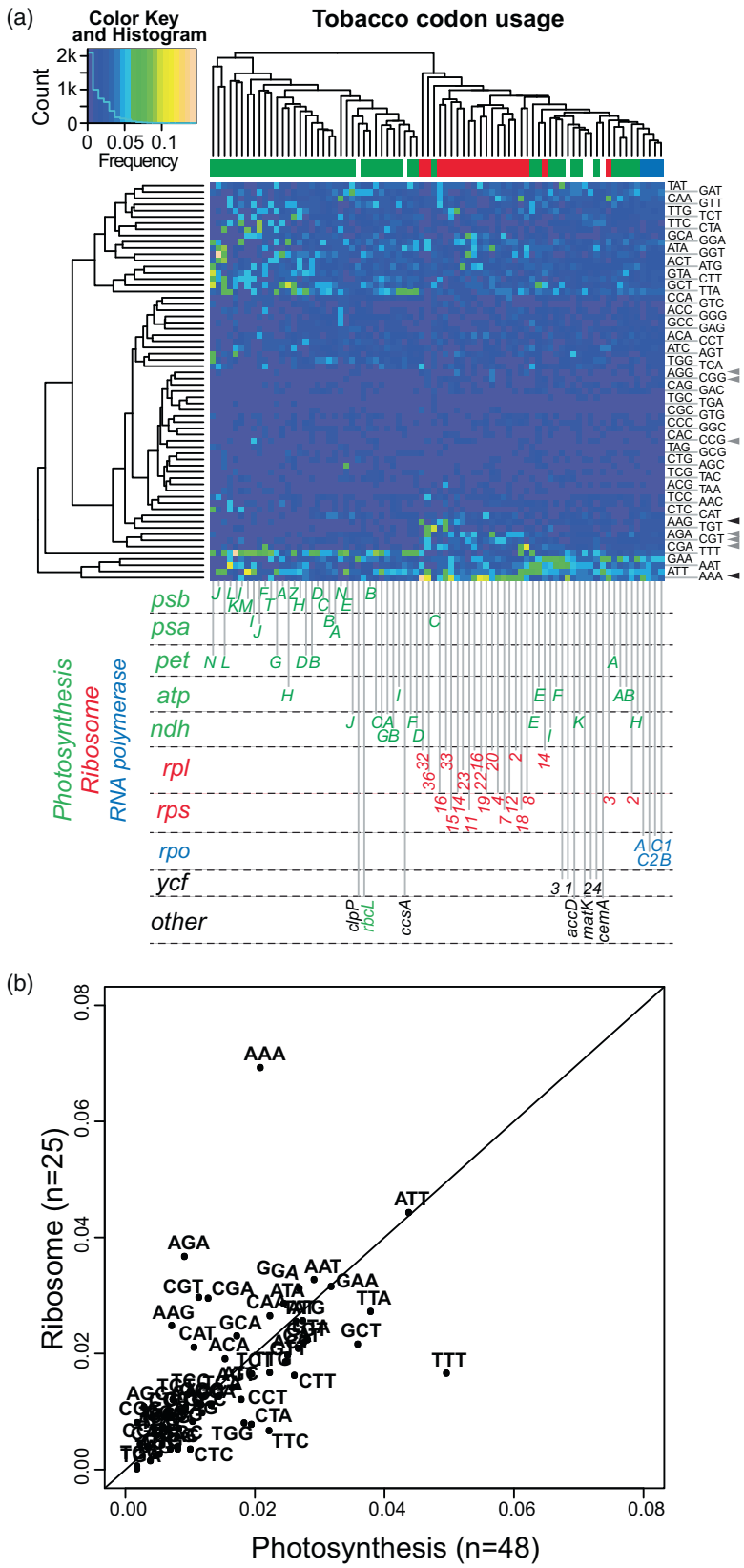

Figure 4. The AAA lysine codon is overrepresented in ribosomal protein genes.
(a) Hierarchical cluster analysis and heat map of the codon usage of each chloroplast gene. Codon bias for each protein-coding gene in the plastid was determined individually by counting the occurrences of each codon within a gene and dividing this number by the gene's total codon count. Chloroplast genes are functionally classified into three groups, photosynthesis, ribosome, and RNA polymerase. Selected codons relevant here are marked: black arrowheads: lysine codons; gray arrowheads: arginine codons.
(b) Comparison of codon frequencies in ribosomal versus photosynthesis genes.

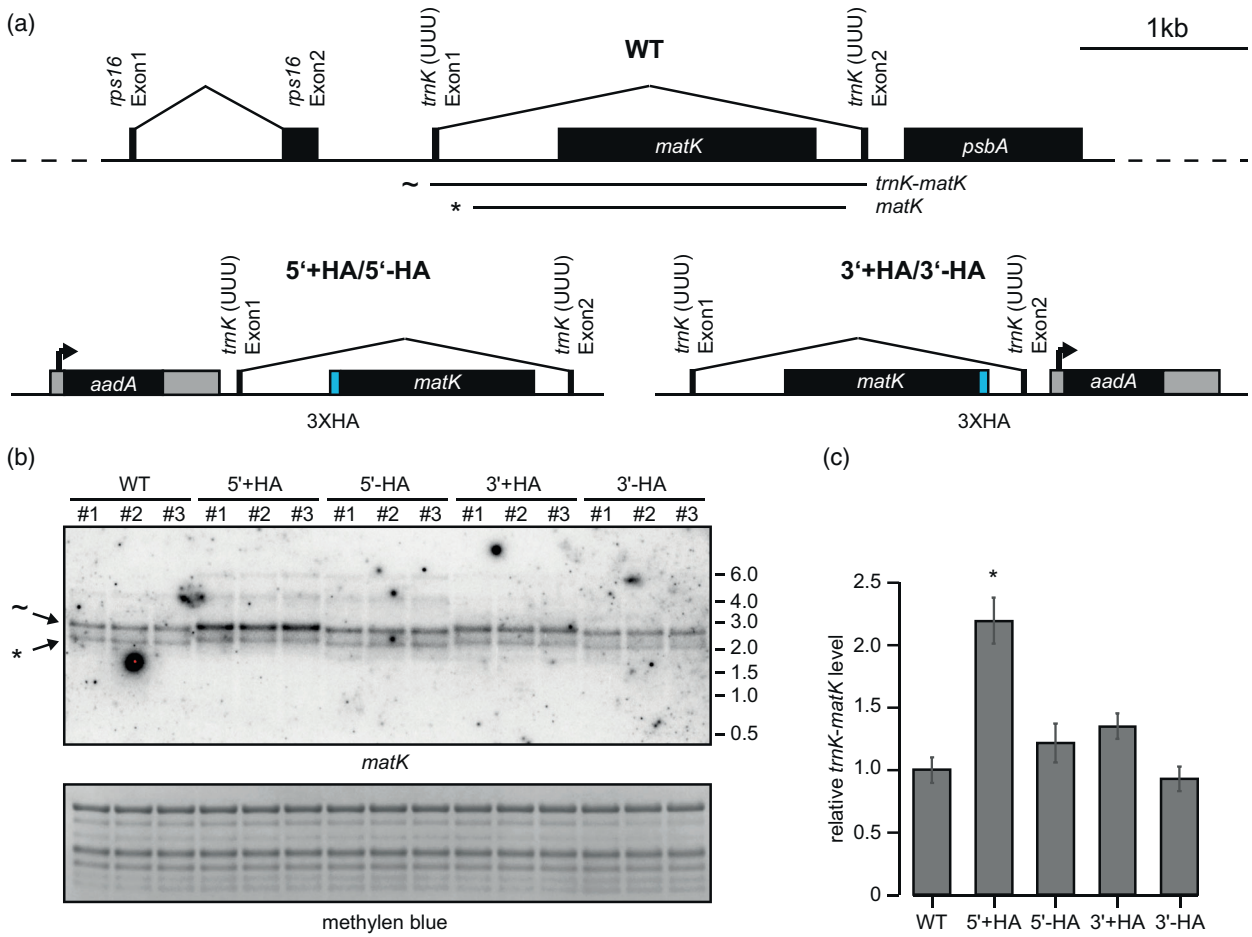

Figure 5. Analysis of unspliced *trnK* precursor transcript levels in transplastomic lines.
(a) Map of the *matK* genomic region in tobacco and a description of the alterations in the four transplastomic lines under investigation. Black boxes correspond to exons, and lines connecting exons correspond to introns. Gray boxes indicate positions of regulatory elements i.e. the tobacco 16S rDNA promoter and 3′UTR of the Chlamydomonas *rbcL* gene. Blue boxes upstream (5′+) or downstream (3′+) of the *matK* open reading frame represent three copies of the hemagglutinin affinity tag (3XHA). 5′- and 3′-lines do not encode for this tag but still contain the *aadA*-cassette (spectinomycin-resistance gene) driven by the strong 16S rDNA promoter. Two different transcripts detected by RNA gel blot analysis representing the unspliced precursor as well as the alternative lariat are indicated (~ and *; the canonical lariat cannot be separated from the precursor in this gel).
(b) RNA gel blot analysis of 3 μg of total tobacco plant RNA from 7 day old plants using a probe directed against the *matK* open reading frame. A methylene blue staining of the membrane before hybridization controls for equal loading. A band corresponding in size to the unspliced *trnK-matK* transcript (~) and a band corresponding to the free *trnK* intron (*) are indicated. We interpret the latter as the non-canonical lariat. Note that the matK versions with 5′- and 3′-extended reading frames migrate slower in the gel than the wild-type and −HA lines. Although 5′+HA lines shows increased accumulation of RNAs, this was not observed for the 5′−HA line, suggesting that the HA-tag itself contributes to the overaccumulation of the precursor, potentially by altering RNA degradation rates.
(c) Quantification of the unspliced *trnK* transcript from the RNA gel blot analysis in b. Signal intensities were normalized against the mean of the three wild-type signals. Shown is the mean ± SD. The significance of differences was calculated using an ANOVA with Tukey HSD (honestly significant difference) post hoc test. 5′+HA lines accumulate a significantly different amount of unspliced *trnK* compared to all other lines ($P < 0.05$).

Next, we investigated whether the overexpression of the precursor also leads to increased levels of the mature tRNA-K. After separating small RNAs from the transplastomic lines via PAGE, we hybridized the blots with probes against tRNA-K and two other tRNAs, tRNA-L-UAA and tRNA-V-UAC (Figure 6a). *trnL* contains a group I

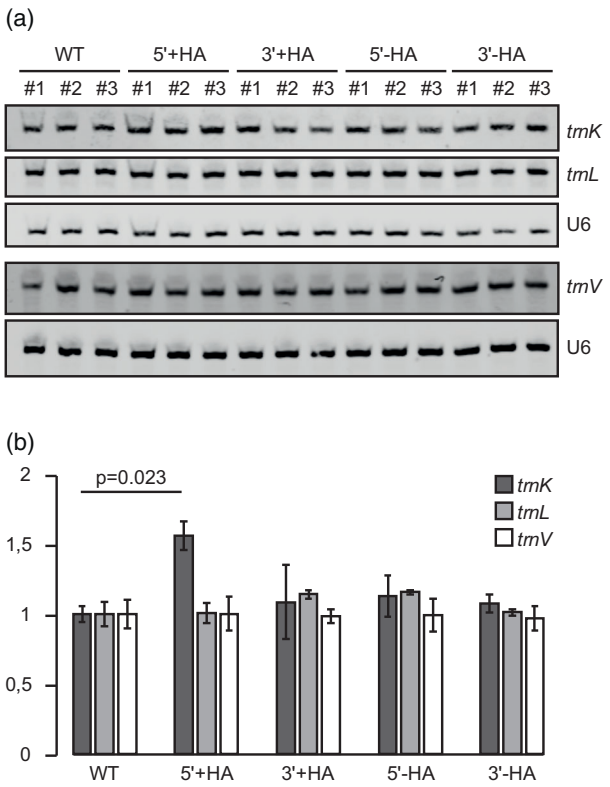

Figure 6. *trnK* over accumulates in the 5′+HA line.
(a) RNA gel blot analysis of selected intron-containing chloroplast tRNAs. 2 μg total RNA was separated on denaturing polyacrylamide gels and transferred to a nylon membrane. Chloroplast tRNAs were probed with fluorescently labeled oligonucleotides complementary to the second exon. A probe detecting U6 snRNA was used as a loading control. This experiment was conducted with three biological replicates (plants #1–3).
(b) Quantification of signal intensities from RNA gel blot analysis in (b). The significance of differences was calculated using an ANOVA with Tukey HSD post hoc test (significance threshold: $P < 0.05$).

intron that does not depend on MatK, whereas *trnV* contains a group IIA intron, but was not significantly enriched in our RIP-Seq experiment (Figure S1). We observed a significant increase in tRNA-K levels relative to wild-type in 5′+HA plants, whereas the abundance of the two other tRNAs remained unchanged across the analyzed genotypes (Figure 6b).

Increased *matK*/tRNA-K(UUU) levels lead to shifts in the translation of photosynthetic versus ribosomal genes

To investigate the impact of increased expression levels of tRNA-K(UUU) in 5′+HA lines on translation, we conducted a ribosome profiling experiment. Using WT plants to normalize the results, we compared 5′+HA plants with 5′−HA plants by subjecting leaf tissue from 14-day-old tobacco plants to ribosome footprint purification, followed by fluorescent dye labeling of the footprints. These labeled footprints were then hybridized to a high-resolution tiling microarray, which covers all chloroplast ORFs, as previously described (Trösch et al., 2018). This process allowed us to map ribosome footprints with a resolution of approximately 30 nucleotides, thanks to the 20-nucleotide overlap of the 50-mers on the array. We averaged the array signals of all probes for chloroplast genes encoding photosynthetic proteins as well as genes encoding ribosomal proteins and compared the distribution of translation scores. Specifically, we measured the fold change in ribosome footprint and total RNA signal between 5′+HA or 5′−HA lines versus WT. We normalized the fold change so all samples have the same distribution across all replicates using the R package *Limma* (Ritchie et al., 2015). We observed a significant up-shift in the ribosomal genes compared to the photosynthetic genes, indicating an overall higher ribosome occupancy on ribosomal protein mRNAs in the *matK/trnK* overexpressor line (5′+HA-line; Figure 7a). To determine whether this shift in ribosome occupancy is caused indirectly by an increase in the respective mRNA levels, we analyzed RNA accumulation by a parallel microarray hybridization experiment. Here, neither the photosynthetic genes nor the genes coding for ribosomal proteins show a change in signal in the overexpressor versus controls (Figure 7b). In conclusion, increasing the expression of *matK/trnK* correlates with an increase in translation of ribosomal protein mRNAs.

DISCUSSION

Translation has emerged as a key point for chloroplast gene regulation (Zoschke & Bock, 2018). It has been found that chloroplast translation rates provide a better representation of the subunit stoichiometry in thylakoid membrane complexes involved in photosynthesis compared to RNA levels (Zoschke et al., 2013; Zoschke & Barkan, 2015). Furthermore, chloroplast translation efficiency responds rapidly to changes in light, temperature and developmental stage (Chotewutmontri & Barkan, 2018, 2020; Gao et al., 2022; Schuster et al., 2020; Trösch et al., 2022). However, the mechanisms underlying translation adjustments are still poorly understood.

So far, very few general mechanisms of translational regulation have been observed in chloroplasts, and all of them are based on similarities to bacterial systems, like ppGpp-based signaling, the role of PSRP1 and redox-regulated translation elongation factor Tu (Gaca et al., 2015; Schröter et al., 2010; Sharma et al., 2010; Sugliani et al., 2016; Vila-Sanjurjo et al., 2004). In addition to these general regulatory mechanisms of translation, there are also factors that are specifically supporting translation of one or few mRNAs (Prikryl et al., 2011; Zhelyazkova et al., 2012; summarized in Zoschke & Bock, 2018), but these do not account for the co-regulation of gene groups at the translational level. Here, we propose a simpler explanation for co-translation of mRNAs, which involves modulating the abundance of a specific tRNA

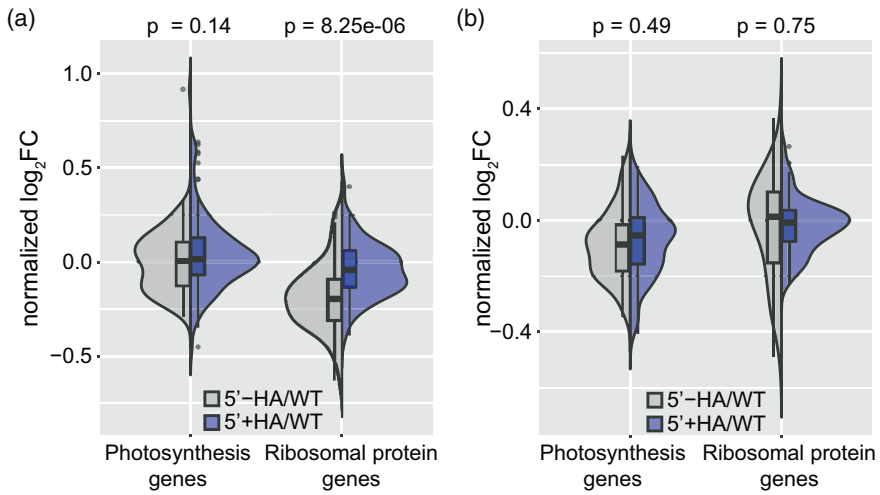

Figure 7. MatK levels correlate with translational changes of ribosomal versus photosynthetic genes.
(a) Comparison of chloroplast ribosomal footprints between *matK/trnK*-overexpressing plants (+HA) and control plants (−HA) in comparison to wild type (wt) using microarray-based RNA profiling. The microarray data were separately analyzed for genes encoding photosynthetic proteins and genes responsible for ribosomal proteins. The *P*-values provided indicate the significance of the difference in footprint accumulation between the overexpressor and control plants for each gene group. Importantly, our analysis revealed a significant difference in ribosome footprints between genes encoding photosynthetic proteins and genes encoding ribosomal proteins when comparing the 5′+HA *matK/trnK* overexpressor lines with the control lines. The analysis is based on three biological replicates for each genotype.
(b) Same analysis as in (a) but for RNA from the same plant lines. Note that genes for ribosomal proteins show no significant increase in RNA levels in the overexpressor for neither photosynthetic nor ribosomal protein genes. The analysis is based on three biological replicates for each genotype.

species that recognizes codons overrepresented in a particular gene group.

We have discovered that the AAA codon is the most biased codon between photosynthesis and ribosomal genes. Increasing the levels of tRNA-K(UUU) in an overexpressor of the *trnK/matK* locus correlated with an elevation of ribosomal protein gene translation, as observed through ribosome profiling. We furthermore note, that other functions of MatK could contribute to driving the translation of ribosomal proteins. MatK is also required for splicing of ribosomal protein mRNAs, such as *rps12* and *rpl2*. It is conceivable that the production of ribosomal proteins via MatK-dependent splicing contributes to an increased translational capacity in the *trnK/matK* over-expressor. To determine the contribution of splicing efficiency of different *matK* targets to the translation enhancement of mRNAs for ribosomal proteins, further investigation is needed, such as ectopic expression of a pre-spliced version of *trnK* to separate its expression from the influence of MatK. At present however, we propose the most simple and parsimonious model that MatK impacts activation of translation of ribosomal mRNAs by supporting canonical lariat formation and thus tRNA-K(UUU) production.

This model is reminiscent of the translation of stress-related genes in yeast that tend to use rare codons (Gingold et al., 2012)—under stress, tRNA pools are skewed toward those tRNAs that recognized rare codons so that stress proteins are translated more efficiently than protein involved in growth and proliferation (Torrent et al., 2018). In general, differential tRNA expression is a well-known phenomenon (Dittmar et al., 2006; van Bortle et al., 2015), but was rarely connected to functional readouts, for example in cancer progression (Goodarzi et al., 2016). This is probably due to the high redundancy of isodecoders in the nucleus, which in most cases prevents a simple genetic approach for functional studies. For example, a knock-out of six tRNA-Phe genes was required to uncover the importance of this isodecoder set for mouse embryo development (Hughes et al., 2023), but at the same time revealed that one particular tRNA-Phe gene was relevant alone for neuronal function (Hughes et al., 2023). Such single-isodecoder effects are however rare. The chloroplast offers the interesting situation of a small, minimal set of tRNAs with little isoacceptor redundancy. Any manipulation of single tRNAs can directly affect translation and compensation by other tRNAs is minimal (Agrawal et al., 2020; Alkatib, Fleischmann, et al., 2012; Alkatib, Scharff, et al., 2012; Legen et al., 2007). The manipulation of tRNA-K by MatK overexpression demonstrates that specific translation changes can be realized by single tRNA species. Whether more tRNA species entail a clear effect on just a subset of chloroplast mRNAs or result in global translational changes, remains to be determined. In this context, it is noteworthy that the codon for phenylalanine, TTT, is significantly overrepresented in genes associated with photosynthesis and that the chloroplast genome encodes only a single tRNA for phenylalanine.

Manipulating the expression of tRNA-F(GAA) and observing its impact on the translation of photosynthetic genes would be a fascinating line of inquiry.

Regulating translation through tRNA-K(UUU) abundance can also resolve the longstanding issue of how genes in mixed operons can be differentially regulated. Unlike bacterial operons, chloroplast operons are typically mixed, meaning that ribosomal protein genes are co-transcribed with photosynthesis genes, as seen in the *psaA/psaB/rps14* operon. Initially, it was believed that the processing of such mixed precursor RNAs into monocistronic forms would determine the eventual translation of an open reading frame. However, polysome analyses and ribosome profiling experiments have demonstrated that the processing state of an mRNA has little impact on the translation rate in most cases (Barkan, 1988; Chotewutmontri & Barkan, 2016; Staub & Maliga, 1995; Zoschke et al., 2013; Zoschke & Barkan, 2015). On the other hand, tRNA-K(UUU) abundance is completely independent of processing state and adjacent ORFs, enabling regulation of ribosomal protein genes across highly diverse contexts and transcripts in a straightforward manner. This could be for instance relevant during leaf development. In meristematic and young leaf tissue, the gene expression apparatus is primarily expressed to prepare for the later production of the photosynthetic machinery (Chotewutmontri & Barkan, 2016). We propose that an early expression of MatK and thus tRNA-K(UUU) during leaf development will contribute to setting up the gene expression apparatus, in particular the ribosome. This temporal separation of the expression of two gene groups is logical as chloroplast translation is particularly crucial during chloroplast biogenesis, i.e. in young tissue. By contrast, once established, the photosynthetic apparatus remains, with very few exceptions, highly stable (Schöttler et al., 2015; Schöttler & Tóth, 2014) and the demand for translational capacity is accordingly low later in development (Chotewutmontri & Barkan, 2016).

Furthermore, it is important to note that plastid translation remains relevant even in the absence of photosynthesis due to the presence of reading frames essential for non-photosynthetic metabolism. One example is *accD*, which encodes an essential enzyme involved in the initial step of fatty acid biosynthesis. Consequently, we predict that in roots and other non-photosynthetic tissues, the expression of *trnK/matK* will contribute to maintaining basal levels of the translational apparatus, ensuring the proper synthesis of proteins necessary for non-photosynthetic metabolic processes. In addition to potential developmental relevance, we present evidence that *trnK* splicing is changed during heat acclimation with more alternative lariats being formed at high temperatures. How this impacts tRNA abundance and translational output during heat response remains to be determined.

MatK as a modifier of alternative lariat formation of the tRNA-K (UUU) precursor RNA has a potential relevance during temperature acclimation

Three routes have been described for group II intron splicing—the canonical branching pathway, the hydrolytic pathway without lariat formation and the circularization pathway (LaRoche-Johnston et al., 2018). None of these routes is compatible with the alternative lariats identified here. In the absence of functional evidence for the alternative splicing products, we hypothesize that the alternative lariat is non-functional, possibly arising due to misfolding of the RNA that is enhanced at higher temperatures. This would be reminiscent of the finding that the circle-to-lariat ratio of the LI.LtrB group II intron from *Lactococcus lactis* is significantly influenced by temperature changes (Monat & Cousineau, 2020) and the general sensitivity of splicing to heat and cold in plants (Dikaya et al., 2021). Alternative lariat formation leading to mis-splicing has been observed in the trans-spliced intron of the *nad5* mRNA in the mitochondria of several plant species (Elina & Brown, 2010). This suggests that such abnormal splicing events may be more widespread in plants. MatK is fostering the canonical splicing pathways as suggested by the correlation of its expression with tRNA-K(UUU) levels in the over-expressor. Our RIP-Seq results furthermore point out that the primary targets within introns are DI and DVI. This is in line with bacterial maturases that are known to deeply penetrate into DI, which supports the intron-binding site (IBS)—exon binding site (EBS) interaction (Qu et al., 2016) and that exert their influence on splicing by engaging in weak interactions with the intron's active site and DVI (Dai et al., 2008; Matsuura et al., 2001). Similar to MatK, bacterial maturases also interact with DVI (Haack et al., 2019; Qu et al., 2016; Xu et al., 2023). This interaction is considered crucial for forming the catalytic center necessary for splicing. DVI is engaged by protein domain X, which is shared between chloroplast and bacterial maturase proteins. Another intron domain, DIV, shows strong co-enrichment with MatK for several introns and is also a well-recognized target of bacterial intron-maturases (Dai et al., 2008; Zhao & Pyle, 2017). It is specifically bound by the RT-0 protein domain of bacterial maturases, a domain absent in MatK, raising intriguing questions about how MatK interacts with DIV. Overall, the data indicate that MatK retains several conserved interaction sites; however, it remains unclear which of its protein domains are involved in these interactions, especially given the significant sequence variation from its bacterial counterparts. In sum, these studies strongly suggest that bacterial maturases play a crucial role in modulating splicing dynamics by directly interacting with key regions within the intron, such as the active site and the branch site adenosine residing in DVI. We hypothesize that MatK acts in a similar manner, which

suppresses the formation of an alternative structure favored at higher temperature that allows the selection of a faulty 5′-splice site. This can be tested by structure probing experiments of the *trnK* intron in the presence and absence of MatK. Our findings indicate that MatK regulates chloroplast gene expression beyond functioning as a general splicing factor, and that control of abundance of specific tRNAs adds an exciting layer to the regulatory hierarchy controlling translation in chloroplasts.

MATERIAL AND METHODS

Plant material

Nicotiana tabacum transplastomic lines expressing Hemagglutinin (HA)-tagged MatK as well as control lines were prepared previously (Zoschke et al., 2010). Plants were grown on soil under long day conditions (16 h light, 8 h dark) at 27°C with light intensities of approximately 300 μmol m^{-2} sec^{-1}. For acquisition of 7-day-old tissue for chloroplast isolation, seeds were sown on polyamide nets (mesh size 500 μM, Franz Eckert GmbH) on soil. Both seed sowing and seedling harvesting were performed at 10:00 am.

Chloroplast isolation and stroma extraction

The procedure of chloroplast isolation from tobacco was modified from a protocol developed for maize (Voelker & Barkan, 1995). Seedlings of 7-day-old tobacco (without roots) were harvested from 3 to 4 plates grown on mesh-covered soil (d = 14 cm) and were homogenized with a waring blender in 350 mL grinding buffer (50 mM HEPES-KOH [pH 8.0], 330 mM Sorbitol, 2 mM EDTA, 1 mM MgCl2, 1 mM $MnCl_2$, 0.25% BSA, 1.5 mM Sodium ascorbate), once for 5 sec at low speed, and twice more for 5 sec at the high-speed setting. Next, the mixture was filtered through one layer of MicroCloth (Calbiochem) and centrifuged at 1000g for 6 min, after which the pellet was resuspended in 1–2 mL of high salt (HS) buffer. After adding 3–4 volumes of HS buffer, it was centrifuged at 1000g for 6 min. The supernatant was discarded again, 200–400 μL EX buffer (0.2 M KAc, 30 mM HEPES-KOH [pH 8.0], 10 mM $MgAc_2$, 2 mM DTT, before use, add 1× protease inhibitor [Protease Inhibitor Cocktail Tablets, Roche], 0.4 mM Phenylmethylsulfonyl fluoride [PMSF], 0.1 μg/mL Aprotinin) was added to the pellet, and the mixture was squeezed through a syringe (needle: 0.55 × 25 mm) ~40 times to lyse chloroplasts. Finally, lysed chloroplasts were centrifuged at 30 000g for 30 min to separate the membrane and stroma fractions. The stroma fraction was used for immunoprecipitation (IP) of MatK.

RIP-Seq

For each MatK co-IP, two volumes of co-IP buffer (Co-IP buffer: 0.15 M NaCl, 20 M Tris–HCl (pH 7.5), 2 mM $MgCl_2$, 0.5% NP-40 (v/v)) and 5 μg of mouse anti–HA antibody (Sigma) were added to the stroma fraction containing approximately 200 μg of protein. The stroma-antibody mixture was rotated at 12 rpm for 1 h, after which 50 μL Magnetic Beads (Life Technologies) were added and the reaction was rotated for one more hour. Next, the beads were pelleted on a magnetic rack, and the supernatant was taken for RNA extraction and Western blot. Finally, the IP pellet was washed 3 times with co-IP buffer, and 200 μL EX buffer was added to the IP pellet before storage or RNA extraction. The same fraction (1/50) was aliquoted from both IP supernatant and pellet for Western blot.

RNA was extracted with Phenol/Chloroform from the IP pellet of HA tagged and control lines. Next, the RNA samples were used for library construction using ScriptMiner Small RNA-seq library preparation Kit (Epicentre) and sequencing was performed on an Illumina NextSeq500.

Mapping

Quality-trimmed Illumina reads from the RIP-seq experiment were mapped to the *N. tabacum* chloroplast genome (NC_001879.2) with the repeat region masked. We utilized CLC Workbench (Version 6.0.1) with the following settings: Mismatch cost: 2; Insertion cost: 3; Deletion cost: 3; Length fraction: 0.5; Similarity fraction: 0.8. Local alignment was applied to enhance accuracy.

RIP-Seq analysis—domain-based peak selection

To identify the preference of MatK for domains of type-2-introns (Michel et al., 1989), we sorted the bases within each domain based on their normalized +HA to −HA ratios and selected the top 40 bases. The mean of the selected bases was used for heatmap generation, utilizing the ComplexHeatmap library (Gu, 2022). Domains were clustered using the Euclidean distance method.

RNA gel blot hybridization

Total RNA was extracted using TRIzol (Invitrogen) following the manufacturer's protocol. Detection of RNAs with radiolabeled probes was performed as described (Kupsch et al., 2012). For detecting RNAs encompassing *trnK* exon sequences, the trnKex2 oligonucleotide (tgggttgcccgggattcgaacccggaactagtcgg, Figure 3a) was directly end-labeled using T4 polynucleotide kinase. For subsequent detection of all intron-containing transcripts, including free introns after splicing, oligonucleotides MatKseqfor1 (gaagttcgataccttgttcc) and matKolrev1 (gataattcgccagatcattgataca) were used for amplifying part of the *matK* reading frame. The resulting PCR product was body-labeled, denatured and hybridized to the stripped RNA gel blot (Figure 3a).

Mature tRNAs were separated by denaturing Urea-PAGE, transferred to nylon membranes and hybridized in ULTRAhyb™-Oligo buffer (Invitrogen). DNA oligonucleotides used as probes were extended with 5-Azido-PEG4-dCTP (Jena Bioscience) and terminal transferase (NEB). Purified extended oligonucleotides were click-labeled with Cyanine5.5 or Cyanine7.5-alkyne (Lumiprobe). Probe sequences for Figure 6(a) were designed for *trnK* exon 2 (trnKex2: tgggttgcccgggattcgaacccggaactagtcgg); *trnV* exon 2 (trnVex2: tagggc tatacggactcgaaccgtagaccttctcg); *trnL* exon 2 (trnLex2: tggggatagaggg acttgaaccctcacgatttttaaagtcgacggatttt); and U6 (aggggccatgctaatcttct ctgtatcgttccaa). For probe generation against *matK* transcripts (Figure 5b). Oligonukleotides matKNt.rp (cattcccgtgactttatgggc) and matKNt.T7 (taatacgactcactatagggaagaagctcgtgggaaggtc) were used to generate PCR fragments that served as templates for *in vitro* transcription reactions in the presence of radio-labeled nucleotides (Figure 5b).

Immunoblot

Immunoblot analyses were performed as described (Qu et al., 2018).

Ribosome profiling

Ribosome profiling started from 7-day-old material and was done as described based on microarray hybridization of an oligonucleotide array covering the entire tobacco chloroplast coding sequence with 50mer oligonucleotides on both strands (Trösch et al., 2018). The data are presented in Supplemental dataset 1.

ACKNOWLEDGMENTS

We thank Ines Gerlach for excellent technical support. This research was supported by the DFG via TR175-A02 to CSL, TR175-C05 to K.K., TR175-D01 to U.O., TR175-A07 to H.R. and TR175-A04 and ZO 302/5-1 to R.Z. Open Access funding enabled and organized by Projekt DEAL.

CONFLICT OF INTEREST STATEMENT

The authors declare no conflict of interest related to the publication of this manuscript.

DATA AVAILABILITY STATEMENT

Sequencing data have been deposited in GEO, accession number GSE245847. Reviewers can access this data using the reviewer token svsryomazdapfal.

SUPPORTING INFORMATION

Additional Supporting Information may be found in the online version of this article.

Figure S1. Structure prediction of putative alternative splicing products of tRNA-K(UUU).

(a) Structure of tobacco tRNA-K(UUU) (Abe et al., 2014). Green = D-loop; yellow = acceptor stem; blue = ψ-loop; brown = anticodon.

(b) Schematic representation of a putative alternative splicing project utilizing an intron-internal 5′-splice site. The position and length of the additional intronic sequence found in such a product is marked in magenta.

(c) Structure prediction of the alternatively spliced product using RNA fold (Lorenz et al., 2011) with default settings. Colour code as in (a) and (b).

Table S1. Top-enriched binding sites of MatK in chloroplast introns.

DataSet S1. Data from array-based ribosome profiling experiments and control hybridizations with total RNA. The table sheets are named according to the harvesting time points of the experiments and the type of analysis (for details see Results and Methods sections). Total RNA and ribosome footprints that derived from control WT plants were labeled with Cy5 and the signals were detected at 635 nm. Total RNA and ribosome footprints that derived from 5′-HA plants were labeld with Cy3 and detected at 532 nm.

REFERENCES

Abe, T., **Inokuchi, H.**, **Yamada, Y.**, **Muto, A.**, **Iwasaki, Y.** & **Toshimichi, I.** (2014) tRNADB-CE:tRNA gene database well-timed in the era of big sequence data. *FrontGenet*, **5**, 114. https://doi.org/10.3389/fgene.2014.00114

Agrawal, S., **Karcher, D.**, **Ruf, S.** & **Bock, R.** (2020) The functions of chloroplast glutamyl-tRNA in translation and tetrapyrrole biosynthesis. *Plant Physiology*, **183**, 263–276.

Alkatib, S., **Fleischmann, T.T.**, **Scharff, L.B.** & **Bock, R.** (2012) Evolutionary constraints on the plastid tRNA set decoding methionine and isoleucine. *Nucleic Acids Research*, **40**, 6713–6724.

Alkatib, S., **Scharff, L.B.**, **Rogalski, M.**, **Fleischmann, T.T.**, **Matthes, A.**, **Seeger, S.** ***et al.*** (2012) The contributions of wobbling and superwobbling to the reading of the genetic code. *PLoS Genetics*, **8**, e1003076.

Barkan, A. (1988) Proteins encoded by a complex chloroplast transcription unit are each translated from both monocistronic and polycistronic mRNAs. *The EMBO Journal*, **7**, 2637–2644.

Barthet, M.M. & **Hilu, K.W.** (2007) Expression of matK: functional and evolutionary implications. *American Journal of Botany*, **94**, 1402–1412.

Barthet, M.M., **Pierpont, C.L.** & **Tavernier, E.-K.** (2020) Unraveling the role of the enigmatic MatK maturase in chloroplast group IIA intron excision. *Plant Direct*, **4**, e00208.

Baumgartner, B.J., **Rapp, J.C.** & **Mullet, J.E.** (1993) Plastid genes encoding the transcription/translation apparatus are differentially transcribed early in barley (*Hordeum vulgare*) chloroplast development (evidence for selective stabilization of psbA mRNA). *Plant Physiology*, **101**, 781–791.

Braukmann, T., **Kuzmina, M.** & **Stefanovic, S.** (2013) Plastid genome evolution across the genus Cuscuta (Convolvulaceae): two clades within subgenus Grammica exhibit extensive gene loss. *Journal of Experimental Botany*, **64**, 977–989.

Chotewutmontri, P. & **Barkan, A.** (2016) Dynamics of chloroplast translation during chloroplast differentiation in maize. *PLoS Genetics*, **12**, e1006106.

Chotewutmontri, P. & **Barkan, A.** (2018) Multilevel effects of light on ribosome dynamics in chloroplasts program genome-wide and psbA-specific changes in translation. *PLoS Genetics*, **14**, e1007555.

Chotewutmontri, P. & **Barkan, A.** (2020) Light-induced psbA translation in plants is triggered by photosystem II damage via an assembly-linked autoregulatory circuit. *Proceedings of the National Academy of Sciences of the United States of America*, **117**, 21775–21784.

Dai, L., **Chai, D.**, **Gu, S.-Q.**, **Gabel, J.**, **Noskov, S.Y.**, **Blocker, F.J.H.** ***et al.*** (2008) A three-dimensional model of a group II intron RNA and its interaction with the intron-encoded reverse transcriptase. *Molecular Cell*, **30**, 472–485.

Delannoy, E., **Fujii, S.**, **Colas des Francs-Small, C.**, **Brundrett, M.** & **Small, I.** (2011) Rampant gene loss in the underground orchid *Rhizanthella gardneri* highlights evolutionary constraints on plastid genomes. *Molecular Biology and Evolution*, **28**, 2077–2086.

Dikaya, V., **El Arbi, N.**, **Rojas-Murcia, N.**, **Nardeli, S.M.**, **Goretti, D.** & **Schmid, M.** (2021) Insights into the role of alternative splicing in plant temperature response. *Journal of Experimental Botany*, **21**, 7384–7403. Available from: https://doi.org/10.1093/jxb/erab234

Dittmar, K.A., **Goodenbour, J.M.** & **Pan, T.** (2006) Tissue-specific differences in human transfer RNA expression. *PLoS Genetics*, **2**, e221.

Drescher, A. (2003) *ycf1, ycf14 und RNA-Edierung: Untersuchungen an im Lauf der Plastidenevolution neu hinzu gewonnenen Genen und Eigenschaften*. PhD, LMU Munich.

Elina, H. & **Brown, G.G.** (2010) Extensive mis-splicing of a bi-partite plant mitochondrial group II intron. *Nucleic Acids Research*, **38**(3), 996–1008.

Emanuel, C., **Weihe, A.**, **Graner, A.**, **Hess, W.R.** & **Börner, T.** (2004) Chloroplast development affects expression of phage-type RNA polymerases in barley leaves. *The Plant Journal*, **38**, 460–472.

Funk, H.T., **Berg, S.**, **Krupinska, K.**, **Maier, U.G.** & **Krause, K.** (2007) Complete DNA sequences of the plastid genomes of two parasitic flowering plant species, *Cuscuta reflexa* and *Cuscuta gronovii*. *BMC Plant Biology*, **7**, 45.

Gaca, A.O., **Colomer-Winter, C.** & **Lemos, J.A.** (2015) Many means to a common end: the intricacies of (p)ppGpp metabolism and its control of bacterial homeostasis. *Journal of Bacteriology*, **197**, 1146–1156.

Gao, Y., **Thiele, W.**, **Saleh, O.**, **Scossa, F.**, **Arabi, F.**, **Zhang, H.** ***et al.*** (2022) Chloroplast translational regulation uncovers nonessential photosynthesis genes as key players in plant cold acclimation. *Plant Cell*, **34**, 2056–2079.

Garcia-Molina, A., **Kleine, T.**, **Schneider, K.**, **Mühlhaus, T.**, **Lehmann, M.** & **Leister, D.** (2020) Translational components contribute to acclimation responses to high light, heat, and cold in Arabidopsis. *iScience*, **23**, 101331.

Gingold, H., **Dahan, O.** & **Pilpel, Y.** (2012) Dynamic changes in translational efficiency are deduced from codon usage of the transcriptome. *Nucleic Acids Research*, **40**, 10053–10063.

Goodarzi, H., **Nguyen, H.C.B.**, **Zhang, S.**, **Dill, B.D.**, **Molina, H.** & **Tavazoie, S.F.** (2016) Modulated expression of specific tRNAs drives gene expression and cancer progression. *Cell*, **165**, 1416–1427.

Grimes, B.T., **Sisay, A.K.**, **Carroll, H.D.** & **Cahoon, A.B.** (2014) Deep sequencing of the tobacco mitochondrial transcriptome reveals expressed ORFs and numerous editing sites outside coding regions. *BMC Genomics*, **15**, 31.

Gu, Z. (2022) Complex heatmap visualization. *iMeta*, **1**, e43. Available from: https://doi.org/10.1002/imt2.43

Haack, D.B., **Yan, X.**, **Zhang, C.**, **Hingey, J.**, **Lyumkis, D.**, **Baker, T.S.** ***et al.*** (2019) Cryo-EM structures of a group II intron reverse splicing into DNA. *Cell*, **178**(3), 612–623.e12.

Hess, W.R., **Hoch, B.**, **Zeltz, P.**, **Hübschmann, T.**, **Kössel, H.** & **Börner, T.** (1994) Inefficient rpl2 splicing in barley mutants with ribosome-deficient plastids. *Plant Cell*, **6**, 1455–1465.

Hirao, T., **Watanabe, A.**, **Kurita, M.**, **Kondo, T.** & **Takata, K.** (2009) A frameshift mutation of the chloroplast matK coding region is associated with chlorophyll deficiency in the *Cryptomeria japonica* virescent mutant Wogon-Sugi. *Current Genetics*, **55**, 311–321.

Hughes, L.A., **Rudler, D.L.**, **Siira, S.J.**, **McCubbin, T.**, **Raven, S.A.**, **Browne, J.M.** ***et al.*** (2023) Copy number variation in tRNA isodecoder genes impairs mammalian development and balanced translation. *Nature Communications*, **14**, 2210.

Kupsch, C., **Ruwe, H.**, **Gusewski, S.**, **Tillich, M.**, **Small, I.** & **Schmitz-Linneweber, C.** (2012) Arabidopsis chloroplast RNA binding proteins CP31A and CP29A associate with large transcript pools and confer cold stress tolerance by influencing multiple chloroplast RNA processing steps. *Plant Cell*, **24**, 4266–4280.

LaRoche-Johnston, F., **Monat, C.**, **Coulombe, S.** & **Cousineau, B.** (2018) Bacterial group II introns generate genetic diversity by circularization and trans-splicing from a population of intron-invaded mRNAs. *PLoS Genetics*, **14**, e1007792.

Legen, J., **Wanner, G.**, **Herrmann, R.G.**, **Small, I.** & **Schmitz-Linneweber, C.** (2007) Plastid tRNA genes trnC-GCA and trnN-GUU are essential for plant cell development. *The Plant Journal*, **51**, 751–762.

Liebers, M., **Grübler, B.**, **Chevalier, F.**, **Lerbs-Mache, S.**, **Merendino, L.**, **Blanvillain, R.** ***et al.*** (2017) Regulatory shifts in plastid transcription play a key role in morphological conversions of plastids during plant development. *Frontiers in Plant Science*, **8**, 23.

Liere, K. & **Link, G.** (1995) RNA-binding activity of the matK protein encoded by the chloroplast trnK intron from mustard (*Sinapis alba* L.). *Nucleic Acids Research*, **23**, 917–921.

Lorenz, R., **Bernhart, S.H. Höner Zu Siederdissen, C.**, **Tafer, H.**, **Flamm, C.**, **Stadler, P.F.**, & **Hofacker, I.L.** (2011) ViennaRNA Package 2.0. *Algorithms for Molecular Biology*, **6**, 1–26. https://doi.org/10.1186/1748-7188-6-26

Matsuura, M., **Noah, J.W.** & **Lambowitz, A.M.** (2001) Mechanism of maturase-promoted group II intron splicing. *The EMBO Journal*, **20**, 7259–7270.

McNeal, J.R., **Arumugunathan, K.**, **Kuehl, J.V.**, **Boore, J.L.** & **Depamphilis, C.W.** (2007) Systematics and plastid genome evolution of the cryptically photosynthetic parasitic plant genus Cuscuta (Convolvulaceae). *BMC Biology*, **5**, 55.

Michel, F. & **Ferat, J.L.** (1995) Structure and activities of group II introns. *Annual Review of Biochemistry*, **64**, 435–461.

Michel, F., **Umesono, K.** & **Ozeki, H.** (1989) Comparative and functional anatomy of group II catalytic introns—a review. *Gene*, **82**, 5–30.

Monat, C. & **Cousineau, B.** (2020) The circle to lariat ratio of the LI.LtrB group II intron from *Lactococcus lactis* is greatly influenced by a variety of biological determinants in vivo. *PLoS One*, **15**, e0237367.

Prikryl, J., **Rojas, M.**, **Schuster, G.** & **Barkan, A.** (2011) Mechanism of RNA stabilization and translational activation by a pentatricopeptide repeat protein. *Proceedings of the National Academy of Sciences of the United States of America*, **108**, 415–420.

Pyle, A.M. (2016) Group II intron self-splicing. *Annual Review of Biophysics*, **45**, 183–205.

Qu, G., **Kaushal, P.S.**, **Wang, J.**, **Shigematsu, H.**, **Piazza, C.L.**, **Agrawal, R.K.** ***et al.*** (2016) Structure of a group II intron in complex with its reverse transcriptase. *Nature Structural & Molecular Biology*, **23**, 549–557.

Qu, Y., **Legen, J.**, **Arndt, J.**, **Henkel, S.**, **Hoppe, G.**, **Thieme, C.** ***et al.*** (2018) Ectopic transplastomic expression of a synthetic MatK gene leads to cotyledon-specific leaf variegation. *Frontiers in Plant Science*, **9**, 1453.

Rambo, R.P. & **Doudna, J.A.** (2004) Assembly of an active group II intron-maturase complex by protein dimerization. *Biochemistry*, **43**, 6486–6497.

Ritchie, M.E., **Phipson, B.**, **Wu, D.**, **Hu, Y.**, **Law, C.W.**, **Shi, W.** ***et al.*** (2015) limma powers differential expression analyses for RNA-sequencing and microarray studies. *Nucleic Acids Research*, **43**, e47.

Schmitz-Linneweber, C., **Williams-Carrier, R.** & **Barkan, A.** (2005) RNA immunoprecipitation and microarray analysis show a chloroplast Pentatricopeptide repeat protein to be associated with the 5′ region of mRNAs whose translation it activates. *The Plant Cell*, **17**(10), 2791–2804.

Schöttler, M.A. & **Tóth, S.Z.** (2014) Photosynthetic complex stoichiometry dynamics in higher plants: environmental acclimation and photosynthetic flux control. *Frontiers in Plant Science*, **5**, 188.

Schöttler, M.A., **Tóth, S.Z.**, **Boulouis, A.** & **Kahlau, S.** (2015) Photosynthetic complex stoichiometry dynamics in higher plants: biogenesis, function, and turnover of ATP synthase and the cytochrome b6f complex. *Journal of Experimental Botany*, **66**, 2373–2400.

Schröter, Y., **Steiner, S.**, **Matthäi, K.** & **Pfannschmidt, T.** (2010) Analysis of oligomeric protein complexes in the chloroplast sub-proteome of nucleic acid-binding proteins from mustard reveals potential redox regulators of plastid gene expression. *Proteomics*, **10**, 2191–2204.

Schuster, M., **Gao, Y.**, **Schöttler, M.A.**, **Bock, R.** & **Zoschke, R.** (2020) Limited responsiveness of chloroplast gene expression during acclimation to high light in tobacco. *Plant Physiology*, **182**, 424–435.

Sharma, M.R., **Dönhöfer, A.**, **Barat, C.**, **Marquez, V.**, **Datta, P.P.**, **Fucini, P.** ***et al.*** (2010) PSRP1 is not a ribosomal protein, but a ribosome-binding factor that is recycled by the ribosome-recycling factor (RRF) and elongation factor G (EF-G). *The Journal of Biological Chemistry*, **285**, 4006–4014.

Small, I., **Melonek, J.**, **Bohne, A.-V.**, **Nickelsen, J.** & **Schmitz-Linneweber, C.** (2023) Plant organellar RNA maturation. *Plant Cell*, **35**, 1727–1751.

Staub, J.M. & **Maliga, P.** (1995) Expression of a chimeric uidA gene indicates that polycistronic mRNAs are efficiently translated in tobacco plastids. *The Plant Journal*, **7**, 845–848.

Sugliani, M., **Abdelkefi, H.**, **Ke, H.**, **Bouveret, E.**, **Robaglia, C.**, **Caffarri, S.** ***et al.*** (2016) An ancient bacterial signaling pathway regulates chloroplast function to influence growth and development in Arabidopsis. *Plant Cell*, **28**, 661–679.

Suzuki, H., **Zuo, Y.**, **Wang, J.**, **Zhang, M.Q.**, **Malhotra, A.** & **Mayeda, A.** (2006) Characterization of RNase R-digested cellular RNA source that consists of lariat and circular RNAs from pre-mRNA splicing. *Nucleic Acids Research*, **34**, e63.

Torrent, M., **Chalancon, G.**, **de Groot, N.S.**, **Wuster, A.** & **Madan Babu, M.** (2018) Cells alter their tRNA abundance to selectively regulate protein synthesis during stress conditions. *Science Signaling*, **11**, eaat6409. Available from: https://doi.org/10.1126/scisignal.aat6409

Trösch, R., **Barahimipour, R.**, **Gao, Y.**, **Badillo-Corona, J.A.**, **Gotsmann, V.L.**, **Zimmer, D.** ***et al.*** (2018) Commonalities and differences of chloroplast translation in a green alga and land plants. *Nature Plants*, **4**, 564–575.

Trösch, R., **Ries, F.**, **Westrich, L.D.**, **Gao, Y.**, **Herkt, C.**, **Hoppstädter, J.** ***et al.*** (2022) Fast and global reorganization of the chloroplast protein biogenesis network during heat acclimation. *Plant Cell*, **34**, 1075–1099.

Turmel, M., **Otis, C.** & **Lemieux, C.** (2005) The complete chloroplast DNA sequences of the charophycean green algae Staurastrum and Zygnema reveal that the chloroplast genome underwent extensive changes during the evolution of the Zygnematales. *BMC Biology*, **3**, 22.

Turmel, M., **Otis, C.** & **Lemieux, C.** (2006) The chloroplast genome sequence of *Chara vulgaris* sheds new light into the closest green algal relatives of land plants. *Molecular Biology and Evolution*, **23**, 1324–1338.

van Bortle, K., **Nichols, M.H.**, **Ramos, E.** & **Corces, V.G.** (2015) Integrated tRNA, transcript, and protein profiles in response to steroid hormone signaling. *RNA*, **21**, 1807–1817.

Vila-Sanjurjo, A., **Schuwirth, B.-S.**, **Hau, C.W.** & **Cate, J.H.D.** (2004) Structural basis for the control of translation initiation during stress. *Nature Structural & Molecular Biology*, **11**, 1054–1059.

Voelker, R. & **Barkan, A.** (1995) Two nuclear mutations disrupt distinct pathways for targeting proteins to the chloroplast thylakoid. *The EMBO Journal*, **14**, 3905–3914.

Vogel, J. & **Börner, T.** (2002) Lariat formation and a hydrolytic pathway in plant chloroplast group II intron splicing. *The EMBO Journal*, **21**, 3794–3803.

Vogel, J., **Börner, T.** & **Hess, W.R.** (1999) Comparative analysis of splicing of the complete set of chloroplast group II introns in three higher plant mutants. *Nucleic Acids Research*, **27**, 3866–3874.

Vogel, J., **Hübschmann, T.**, **Börner, T.** & **Hess, W.R.** (1997) Splicing and intron-internal RNA editing of trnK-matK transcripts in barley plastids: support for MatK as an essential splice factor. *Journal of Molecular Biology*, **270**, 179–187.

Wolfe, K.H., **Morden, C.W.** & **Palmer, J.D.** (1992) Function and evolution of a minimal plastid genome from a nonphotosynthetic parasitic plant.

Proceedings of the National Academy of Sciences of the United States of America, **89**, 10648–10652.

Xu, L., **Liu, T.**, **Chung, K.** & **Pyle, A.M.** (2023) Structural insights into intron catalysis and dynamics during splicing. *Nature*, **624**(7992), 682–688.

Zhang, X., **Zhang, Y.**, **Wang, T.**, **Li, Z.**, **Cheng, J.**, **Ge, H.** ***et al.*** (2019) A comprehensive map of intron branchpoints and lariat RNAs in plants. *Plant Cell*, **31**, 956–973.

Zhao, C. & **Pyle, A.M.** (2017) Structural insights into the mechanism of group II intron splicing. *Trends in Biochemical Sciences*, **42**, 470–482.

Zhelyazkova, P., **Hammani, K.**, **Rojas, M.**, **Voelker, R.**, **Vargas-Suarez, M.**, **Börner, T.** ***et al.*** (2012) Protein-mediated protection as the predominant mechanism for defining processed mRNA termini in land plant chloroplasts. *Nucleic Acids Research*, **40**, 3092–3105.

Zoschke, R. & **Barkan, A.** (2015) Genome-wide analysis of thylakoid-bound ribosomes in maize reveals principles of cotranslational targeting to the thylakoid membrane. *Proceedings of the National Academy of Sciences of the United States of America*, **112**, E1678–E1687.

Zoschke, R. & **Bock, R.** (2018) Chloroplast translation: structural and functional organization, operational control, and regulation. *Plant Cell*, **30**, 745–770.

Zoschke, R., **Liere, K.** & **Börner, T.** (2007) From seedling to mature plant: Arabidopsis plastidial genome copy number, RNA accumulation and transcription are differentially regulated during leaf development. *The Plant Journal*, **50**, 710–722.

Zoschke, R., **Nakamura, M.**, **Liere, K.**, **Sugiura, M.**, **Börner, T.** & **Schmitz-Linneweber, C.** (2010) An organellar maturase associates with multiple group II introns. *Proceedings of the National Academy of Sciences of the United States of America*, **107**, 3245–3250.

Zoschke, R., **Watkins, K.P.** & **Barkan, A.** (2013) A rapid ribosome profiling method elucidates chloroplast ribosome behavior in vivo. *Plant Cell*, **25**, 2265–2275.